Universal Journal of Electrochemistry
https://ojs.wiserpub.com/index.php/UJEC/

Research Article

Determination and Comparison of Kinetic and Diffusion Parameters from Cyclic Voltammetry of $LaCl_3$ in Eutectic LiCl-KCl

Michael Shaltry[1,5,*], Kerry N. Allahar[2,5], Supathorn Phongikaroon[3,5], Darryl P. Butt[4,5], Michael F. Simpson[4,5]

[1] Idaho National Laboratory, 2525 Fremont Ave., Idaho Falls, Idaho 83415, USA.
[2] Materials and Science Engineering Department, Boise State University, 1910 University Blvd., Boise, Idaho 83725, U.S.A.
[3] Department of Mechanical and Nuclear Engineering, Virginia Commonwealth University. 401 West Main Street, P.O. Box 843015, Richmond, Virginia 23284-3067, USA.
[4] Department of Materials Science and Engineering, University of Utah, 115 South 1460 East, Salt Lake City, Utah 84112, USA.
[5] Center for Advanced Energy Studies, 995 University Blvd., Idaho Falls, Idaho 83401, USA.
E-mail: michael.shaltry@inl.gov

Received: 17 December 2022; **Revised:** 3 March 2023; **Accepted:** 14 March 2023

Abstract: Electrochemical measurements of $LaCl_3$ were obtained in eutectic LiCl-KCl at 773 K. Cyclic voltammetry data were acquired using a tungsten electrode $LaCl_3$ amounts in the molten salt in the range of 0.5 to 3.0 wt%. Both cyclic voltammetry and Tafel analyses of the data resulted in calculation of values for the charge transfer coefficient (0.262), diffusion coefficient (1.67×10^{-5} cm^2 s^{-1}), exchange current density (0.0148 to 0.0473 A cm^{-2}), and charge transfer resistance (0.404 to 1.99 Ω) related to lanthanum ions in the molten salt. Calculated values were compared to those available in the literature. The values of parameters found in literature varied significantly in comparison to those in the present study due to dissimilar experimental conditions, e.g., electrode material, temperature, and $LaCl_3$ concentration.

***Keywords*:** eutectic LiCl-KCl, lanthanum chloride, diffusion coefficient, exchange current density

1. Introduction

Electrochemical methods of characterization are common due to their relative ease of equipment set-up and fast data acquisition. Standard electrochemical measurement techniques (transient in nature) include, but are not limited to, electrochemical impedance spectroscopy (EIS), square wave voltammetry (SWV), chronopotentiometry (CP), chronoamperometry (CA), and cyclic voltammetry (CV).[1] In terms of analysis, CV and CP data are useful to determine physical parameters via equations that are derived from such principles as diffusion (Berzins-Delahay) and electrochemical reaction kinetics (Bulter-Volmer). Semi-integration (SI) is yet another method used extensively to calculate the diffusion coefficient values. These electrochemical methods are useful for many applications, one of which is the high-temperature molten salt systems associated nuclear fuel reprocessing.

Pyroprocessing is an established technology used to treat either metallic or ceramic nuclear fuel [2,3]. This technology was originally developed to process irradiated metallic fuel, such as that from the Experimental Breeder Reactor II, and represented the material recovery component of the Integral Fast Reactor concept [4]. The electrorefiner, which is operated at 773 K and is the crucial unit of the treatment process, is used for recovery of

DOI: https://doi.org/10.37256/ujec.1120232252

useful material from irradiated fuel to manufacture new fuel elements. During electrorefining, lanthanide and actinide fission products are among those that accumulate in the molten eutectic LiCl-KCl (ClLiK) electrolyte, which is the supporting electrolyte.

Due to its prevalence as a fission product [5], the removal of lanthanides from the molten salt [6], and the efforts related to the separation of actinides from lanthanides [7]; lanthanum chloride was chosen for this electrochemical study as a representative of the lanthanide fission product chlorides (e.g., $NdCl_3$ and $CeCl_3$) that exist in the electrorefiner electrolyte. Physical and electrochemical reaction properties, such as the diffusion coefficient and exchange current density, of ionic species that accumulate in the electrorefiner salt are important to determine as they have bearing on process monitoring as well as efforts to model the system. It is important to note that experiments and analyses of $LaCl_3$ in ClLiK under varying conditions have been reported previously (e.g., working electrode material, electrochemical technique, temperature, and concentration of the analyte) [8–16]. All the previously mentioned electrochemical techniques have been used in literature to analyze data of $LaCl_3$ in ClLiK, resulting in estimates of the activity coefficient [15,17], reaction rate constant [18,19], charge transfer coefficient [18,19], as well as the diffusion coefficient and exchange current density. With respect to electrode materials, studies of such liquid cathodes as lead [6], cadmium [20], bismuth [21], gallium [22], and a gallium-indium alloy [23] as well as studies of the reactive electrode material, such as aluminum [24,25], have been performed to assess the separability or co-reduction of lanthanum from other elements. Inert solid metals are more commonly utilized for tests in molten salt, and Table 1 summarizes tests performed using tungsten and molybdenum as working electrodes.

Table 1. Summary of reported diffusion coefficients for $LaCl_3$ in ClLiK with pertinent experimental conditions.

Reference	wt% $LaCl_3$	Temperature (K)	Working Electrode	Method	Diffusion Coefficient $D \times 10^5$ cm^2 s^{-1}
Castrillejo et al. [8]	1.22	773	Tungsten	CP	1.29
Tang and Pesic [9]	1.66	763	Molybdenum	CP	2.10
Lantelme and Berghoute [10]	0.42–2.10	773	Tungsten	CP	2.02
Rappleye et al. [11]	0.85–0.97	773	Molybdenum	CV	1.08 & 1.48
Gao et al. [12]	1.17	773	Molybdenum	CP	1.85
Picard et al. [13]	4.91	723	Tungsten	SI	0.72
Masset et al. [14]	2.99	733	Tungsten	CP	0.8
Vandarkuzhali et al. [15]	1.13	748	Tungsten	CV	1.31
Matsumiya and Matsumoto [16]	-	773	Tungsten	CV	2.1

Although there are several reported values for the diffusion coefficient (D) of $LaCl_3$, which are based on tests with inert working electrodes, the method to calculate D differ by electrochemical technique, determination of reversibility, and equation used for computation. Furthermore, only two of the publications [8,10] listed in Table 1 were produced with experimental conditions mostly consistent with those reported in the present study. Similarly, there are few estimates of the exchange current density and charge transfer resistance in the literature. It is this wide variability of experimental and analytical approaches as well as the limited availability of certain parameters that has motivated the analysis of CV data in a range of $LaCl_3$ concentrations to determine the given parameters with respect to a tungsten electrode.

The objective of this work was to perform electrochemical experiments of ClLiK salt with varying amounts of $LaCl_3$ and use the data obtained to calculate the values of the charge transfer coefficient, diffusion coefficient, exchange current density, and charge transfer resistance. Analysis was primarily focused on determining these parameters and comparing them to those found in literature. The sets of data were generated by recording multi-cycle CV measurements in a relatively large range of scan rates at each of the $LaCl_3$ concentrations. By analyzing specific relationships between the peak current (mass transfer-controlled phenomena), peak potential, and scan rate; the appropriate equation was selected and then used to calculate the diffusion coefficient. The exchange current density and charge transfer resistance were estimated from the Tafel plot (logarithm of current density vs. overpotential) based on a charge transfer controlled region of the CV plot. Due to the availability of many values, the average, standard deviation, and coefficient of variation were calculated.

2. Experimental

Experiments were conducted in an MBraun glovebox containing an argon atmosphere with H_2O and O_2 concentrations less than 5 ppm. A Kerr Lab Electro-Melt furnace in the glovebox was used to heat the molten

salts to 773 K ± 1 K. Anhydrous ClLiK (99.99 % pure, AAPL) was used as the supporting electrolyte, to which ultra-dry $LaCl_3$ (99.99 % pure, Alfa Aesar) was added. The molten salt mixtures were contained by glassy carbon crucibles (HTW Germany, GAT19). Molar concentrations of $LaCl_3$ in 80.0 g of LiCl-KCl were calculated to be 0.330, 0.669, 1.17, 1.63, and 2.06 × 10^{-4} mol cm^{-3} (0.5, 1.0, 1.7, 2.4, and 3.0 wt%). The concentration of $LaCl_3$ will be discussed in terms of weight fraction as a percentage (wt%) in the remainder of this manuscript.

The three-electrode assembly consisted of a working, counter, and reference electrode. The working electrode (WE) was a 2.0 mm diameter tungsten rod (99.95 % pure, Alfa Aesar) and the counter electrode (CE) was a 3.0 mm diameter glassy carbon rod (HTW Germany). A reference electrode (RE) was constructed using a Pyrex tube (10 mm outside diameter and 1.0 mm wall thickness), to which a Pyrex rod was attached. One end of a 1.0 mm diameter silver wire (99.9 % pure, Acros Organics) was made into a spiral sufficiently small in diameter to be inserted into the Pyrex tube. 0.135 g of ultra-dry AgCl beads (99.997 % pure, Alfa Aesar) and 1.00 g of the LiCl-KCl eutectic were placed in the Pyrex tube. Upon melting, a 5.0 mol% AgCl mixture was obtained that served as the RE.

The electrode assembly was made by tying together the WE, CE, and RE with stainless steel wire; each was sheathed with an alumina tube to prevent short circuiting. An alumina-sheathed type-K thermocouple, integrated with the electrode assembly, in direct contact with the salt monitored the salt temperature. The tungsten WE was secured in the alumina tube such that 14 mm of the rod length (l) was immersed. Alumina paste sealed the space between the tungsten and alumina tube. The surface area ($\pi r^2+2\pi rl$ = 0.911 cm^2) of the WE was estimated by geometry. The CE was not secured in the alumina tube and was allowed to contact the bottom of the crucible, effectively making the entire crucible the CE. An illustration of the electrochemical cell can be viewed in a previous publication [26], which has an identical configuration. CV experiments were conducted using a Princeton Applied Research VersaSTAT 4-400 potentiostat coupled to a laptop computer utilizing VersaStudio software. The working electrode was subjected to a CP technique to clean the WE surface of residual lanthanum metal. *iR* compensation was not applied to the measurement routine due to low solution resistance (~ 0.35 Ω as measured by impedance technique) and small currents. Connections between the electrochemical cell and the potentiostat were made via electrical feed-through fittings on the glovebox.

3. Theory and Calculations

The Tafel approximation of the Butler-Volmer equation is valid under when the reaction at the electrode/electrolyte interface is controlled by charge transfer, the cathodic overpotential is relatively large, and the anodic current is negligible which is expressed as

$$i = -i_0 \, exp\left[-\frac{n\alpha F}{RT}\eta\right] \tag{1}$$

where i is the measured current density (A cm^{-2}), i_0 is the exchange current density (A cm^{-2}), α is the charge transfer coefficient, n is the number of electrons transferred in the oxidation/reduction reaction under consideration, F is the Faraday constant (96485 C mol^{-1}), R is the universal gas constant (8.314 J K^{-1} mol^{-1}), T is temperature (K), and η is the overpotential (V) [27]. Equation 1 is useful when applied to the region of a CV, following the cathodic potential sweep during which lanthanum ions are reduced and deposited onto the tungsten electrode. Shown by Figure 1a, reversing the scan (the anodic sweep) causes deposited lanthanum metal to oxidize while the electrode remains at potentials less than the reduction onset potential. Under the conditions of oxidation and reduction, the net current transitions from cathodic, to zero (equilibrium), and then anodic. The justification for assuming charge transfer controlled reaction is shown in the Results and Discussion section.

The potential at which the net current is zero is taken to be the equilibrium potential (E_{eq}) which is necessary to calculate the overpotential ($\eta = E - E_{eq}$). This method is used to prepare the Tafel plot ($log|i|$ vs. η) and is shown by Figure 1b. This method of analysis utilizing CV has been demonstrated previously in literature [28–30]. The exchange current density is calculated by fitting a line to the cathodic side of the Tafel plot for which η > 0.050 V, which is $log|i|$ vs. η, and the intercept of the line is equated to a rearranged form of Equation 1 yielding i_0. At relatively low overpotentials (η < 0.010 V), the inverse of the slope in this region of the CV was taken to be the charge transfer resistance (R_{ct}) and was calculated via Equation 2.

$$R_{ct} = \frac{\Delta\eta}{\Delta i} \tag{2}$$

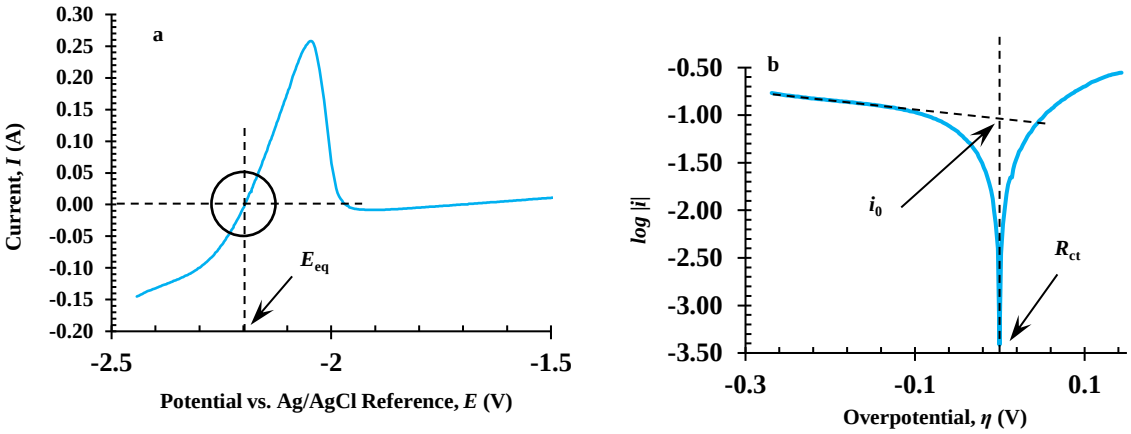

Figure 1. Illustration of a) the anodic sweep of a CV and b) Tafel data used to obtain values of E_{eq}, R_{ct}, and i_0. The data was taken from the 1.7 wt% $LaCl_3$ test with a scan rate (v) equal to 0.5 V s^{-1}.

A soluble-insoluble reaction that displays irreversible characteristics is described by the following equation.

$$I_p = -0.496nFAC\left(\frac{\alpha nF\nu D}{RT}\right)^{\frac{1}{2}} \quad (3)$$

where I_p is the peak current (A), A is the geometric surface area of the WE (cm^2), ν is the scan rate (V s^{-1}), C is concentration (mol cm^{-3}), and D is the diffusion coefficient (cm^2 s^{-1}) [27]. Justification for the use of Equation 3 is provided in the Results and Discussion section.

4. Results and Discussion

A CV of the ClLiK was obtained prior to adding any amount of $LaCl_3$. The expected features of the CV, namely lithium redox peaks (left of CV) and anodic current indicating chlorine evolution (right of CV) are observed, which demonstrates the electrochemical system was functioning as expected. Within the electrochemical window (-2.51–1.1 V), there were no unexpected anodic or cathodic peaks, thus indicating the electrolyte was free of contaminants, as shown by Figure 2.

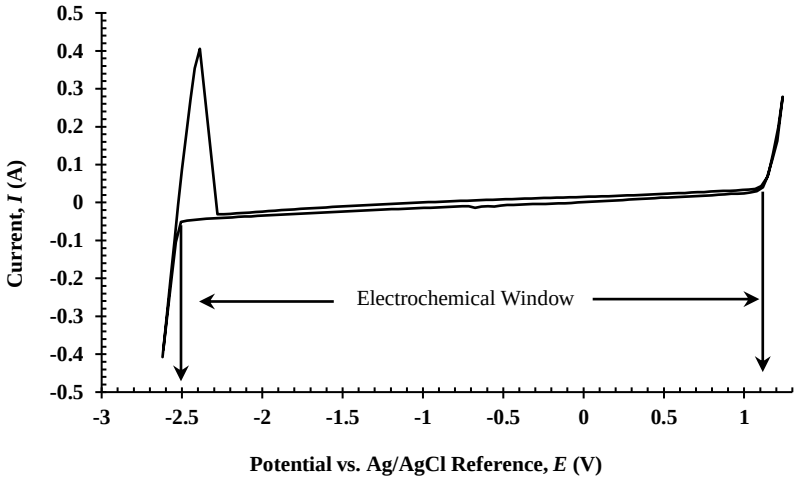

Figure 2. Cyclic voltammogram of ClLiK at 773 K. The scan rate was 0.1 V s^{-1} and the WE was tungsten.

At each concentration of $LaCl_3$, multicycle CV measurements consisting of four cycles were recorded at each of the scan rates and all calculations were based on the second, third, and fourth cycle. CVs acquired after adding the prescribed amounts of $LaCl_3$ displayed (Figure 3) an increase in the magnitude of the redox couple peaks as expected and a shift of anodic and cathodic peak potentials (positive and negative, respectively) was observed. The recorded cathodic peak currents (I_{pc}) were in the range from -0.091 to -0.375 A, and peak potentials (E_{pc}) from -2.28 to -2.35 V.

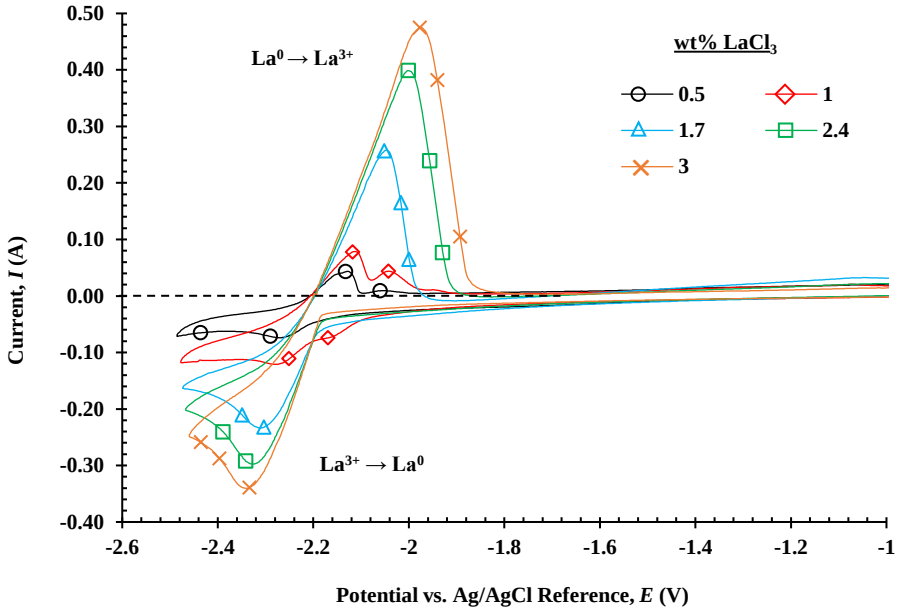

Figure 3. CV plots at 0.5, 1.0, 1.7, 2.4, and 3.0 wt% $LaCl_3$ in ClLiK at 773 K. The scan rate for all curves shown was 0.5 V s^{-1}.

Figure 4 displays CV plots at various scan rates acquired with 1.7 wt% $LaCl_3$ and is representative of measurements at the other concentrations. As expected, the current peaks increase linearly with scan rate. An additional observation to note was the convergence of the five plots in the region of the anodic sweep near E_{eq}. Here, the measured current is independent of scan rate, which implies the electrode process is controlled by charge transfer. [30] Furthermore, a similar feature is shown in Figure 3, which shows the measured current is independent of $LaCl_3$ concentration. It is these observations that provide confidence the electrode reaction in that region is controlled by charge transfer and not mass transfer.

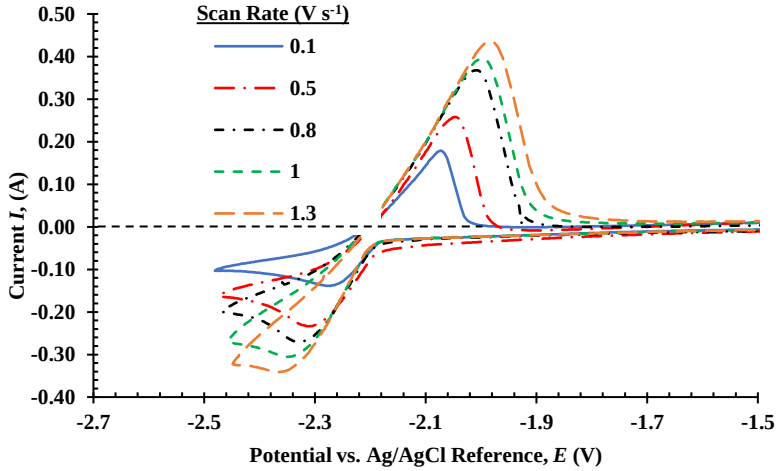

Figure 4. CV plots acquired with 1.7 wt% $LaCl_3$ in ClLiK at 773 K at various scan rates.

To choose the correct equation to calculate D, evaluation of the relationship between I_{pc} and E_{pc} was performed. A plot of peak cathodic current vs. square root of scan rate (as shown in Figure 5) showed a linear functional relationship, indicating the transport of ions to the electrode surface was controlled by diffusion. The dependence of the peak potential on scan rate was more apparent with increasing concentration of $LaCl_3$, as shown in Figure 6. At 0.5 and 1.0 wt% the dependence is small whereas at the higher concentrations it is clearly larger. Due to this observation, the electrochemical reaction was determined to be irreversible. A baseline correction,

described in a previous publication [29], of the peak current was performed to isolate the Faradaic component of the measured current attributable to lanthanum ion reduction, which includes capacitive charging at the electrode-electrolyte interface (also termed residual or non-Faradaic current).

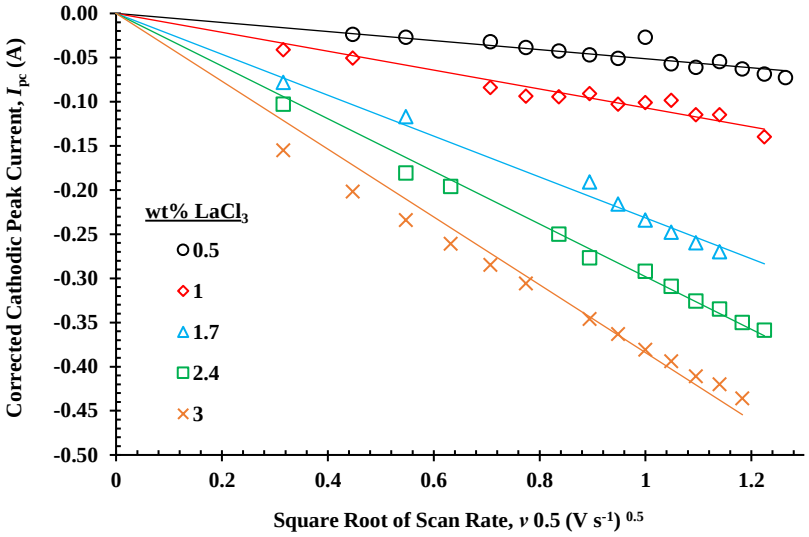

Figure 5. Cathodic peak current (I_{pc}) versus the square root of scan rate ($\nu^{0.5}$) with the $LaCl_3$ concentration as a parameter.

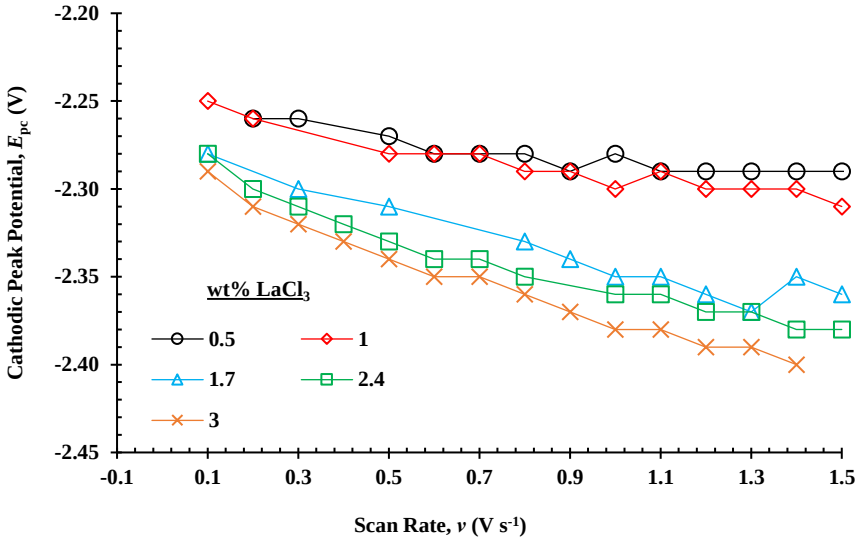

Figure 6. Cathodic peak potential (E_{pc}) vs. the scan rate (ν) with the $LaCl_3$ concentration as a parameter.

In the process of performing the Tafel analysis, the value of α was estimated. Table 2 lists the range, average (μ), standard deviation (σ), coefficient of variation ($c_v = \sigma\,\mu^{-1}$), and number of values (N) upon which the statistical parameters were based, related to α for each concentration of $LaCl_3$. In general, the value of α increases with $LaCl_3$ concentration and is within the range of 0.204 to 0.292. The overall values of $\mu \pm \sigma$ and c_v (N = 201) are (0.262 ± 0.0428) and 0.163, respectively.

Table 2. List of the range, average (μ), standard deviation (σ), coefficient of variation (c_v), and number of values (N) for the charge transfer coefficient (α) at the various concentrations of $LaCl_3$.

wt% $LaCl_3$	0.5	1.0	1.7	2.4	3.0
Range	0.163-0.233	0.202-0.273	0.227-0.316	0.170-0.337	0.247-.380
μ	0.204	0.248	0.285	0.277	0.292

σ	0.0180	0.0161	0.0239	0.0282	0.0316
c_v	0.0882	0.0649	0.103	0.102	0.108
N	42	39	33	42	45

Table 3 lists the statistical parameters for D at each concentration of $LaCl_3$. The values of $\mu \pm \sigma$ and c_v (N = 201) are (1.62 ± 0.477) × 10^{-5} cm^2 s^{-1} and 0.294, respectively. Figure 7 displays the average value of D at each concentration, which are based on CVs at the varying scan rates. For each of the data points in the series, the error bars indicate the standard deviation of values. The trend observed is D increases slightly as a function of $LaCl_3$ concentration.

Table 3. List of the range, average (μ), standard deviation (σ), coefficient of variation (c_v), and number of values (N) for D × 10^5 cm^2 s^{-1} at the various concentrations of $LaCl_3$.

wt% $LaCl_3$	0.5	1.0	1.7	2.4	3.0
Range	0.324-2.22	0.809–2.90	0.990–2.65	0.721–2.54	1.11–4.97
μ	1.52	1.52	1.66	1.66	1.77
σ	0.342	0.393	0.305	0.423	0.506
c_v	0.225	0.259	0.271	0.255	0.286
N	42	39	33	42	45

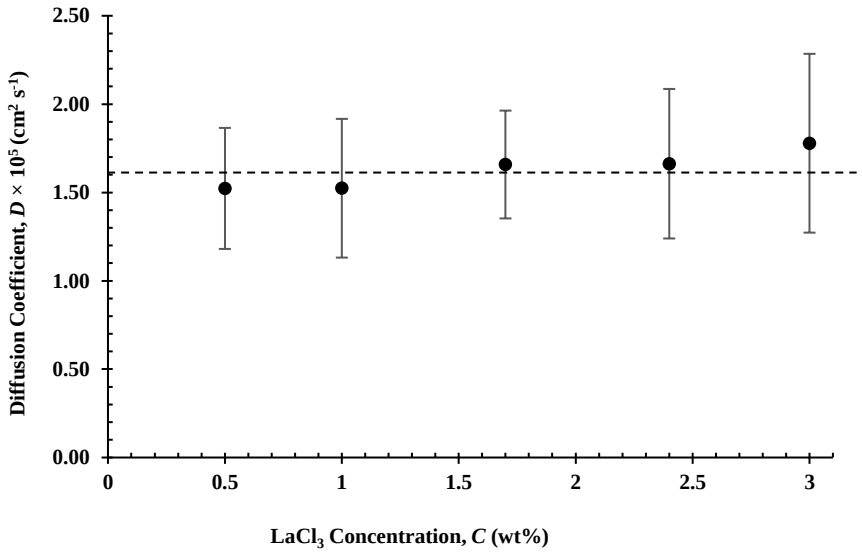

Figure 7. Diffusion coefficient (D) vs. concentration of $LaCl_3$ in ClLiK at 773 K. The error bars indicate standard deviation, and the dashed line indicates the overall average.

The value of the diffusion coefficient, obtained in the present study, was compared with values reported in the literature. As a direct comparison was not possible due to differences in $LaCl_3$ concentration (C) and experimental temperature (T), a method to make the comparison was sought. Based on Equation 3, the relationship DT^{-1} vs. C^{-2} was chosen and is illustrated by Figure 8.

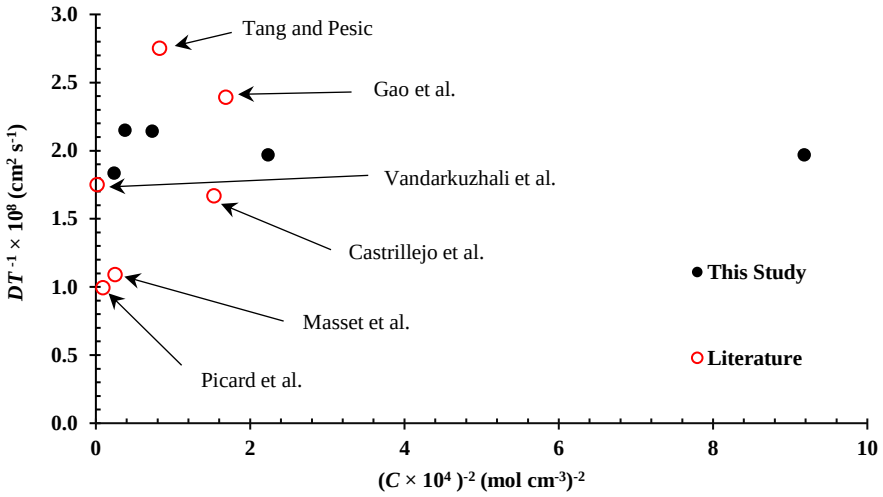

Figure 8. Comparison of results from the present study and literature. $DT^{-1} \times 10^8$ vs. $(C \times 10^4)^{-2}$ is plotted to account for differences in $LaCl_3$ concentration, experiment temperature, and the calculated diffusion coefficient.

An inspection of Figure 8 reveals no discernible trend between the values from the present study and the literature. One might expect the data generated using differing electrodes, such as molybdenum (Tang and Pesic [9] and Gao et al. [31]), to be dissimilar compared to that of tungsten, and this was the case. Furthermore, although a tungsten electrode was used in this study, differences in the magnitude of D was observed, depending on the method used to calculate the value (Lantelme and Berghoute. [10], Picard et al. [13], and Masset et al. [14]), which is noted. Of the entries listed in Table 1, the data produced by Vandarkuzhali et al. [15] using a tungsten electrode and calculation of D using CV data appears to closely match that of the present study. The observed difference in values is assumed to be due to variation of materials, experimental conditions (electrode geometry and electrode spacing), methods of analysis, and electrode surface preparation combined with the true active surface area of the electrode.

As mentioned in the Theory and Calculations section, the value of E_{eq} was necessary as part of the method to estimate i_0. Thus, a value of E_{eq} is calculated for each CV cycle at every scan rate and for all the concentrations of $LaCl_3$ (201 in total). Interestingly, the extreme spread (the difference between the maximum and minimum values) of E_{eq} was low with overall values of $\mu \pm \sigma$ and $|c_v|$ equalling -2.20 ± 0.00487 V and 0.00221, respectively. This small distribution in values of E_{eq} was observed despite several days at the operating temperature and using the same electrode assembly for all measurements.

The values of i_0, with standard deviations as error bars, monotonically increased with $LaCl_3$ concentration as shown in Figure 9. This observation was consistent with expectations. Average values range from 0.0148 to 0.474 A cm^{-2} and are summarized in Table 4. In a situation similar to that of the diffusion coefficient, values of i_0 in the literature arise from electrochemical cells of varying construction. Such factors as temperature, electrode material, effective surface area and preparation, and analyte concentration determine the magnitude of i_0 and were in the range of 10^{-3} to 10^{-1} A cm^{-2}, with most values being on the order of 10^{-2} A cm^{-2}. Yin et al. [32] utilized a liquid bismuth WE at 773 K to estimate i_0 by galvanostatic pulse and EIS techniques, which resulted in a value of 0.0914 A cm^{-2} for both, close to the values determined in the range of concentrations from the present study. Han et al. [6] used a liquid lead WE at temperatures from 853 to 928 K and calculated i_0 via linear polarization (LP) and Tafel methods. By an extrapolation of the i_0 vs. T data, the values of i_0 at 773 K based on the LP and Tafel methods were observed to be within the low range of values in the present study: 0.0329 and 0.0262 A cm^{-2}, respectively. Tang and Pesic [9] used a molybdenum WE to acquire LP measurements, which resulted in a relatively low value of i_0 (0.034 A cm^{-2}) at 773 K. Andrews and Phongikaroon [33] performed a series of electrochemical experiments with $LaCl_3$ concentration from 1.0 to 2.5 wt% and from 723 to 798 K. Using LP, Tafel, and CV methods, they were able to generate functional relationships between i_0 and T. Their results were systematically lower than those in the present study with values of i_0 at 1.0, 1.5, 2.0, and 2.5 wt% (0.134, 0.249, 0.034, and 0.0408 A cm^{-2}, respectively). Lim and Yun [34] also used a tungsten WE and reported i_0 at 1.0 wt% $LaCl_3$ and 773 K as 0.0777 A cm^{-2}, which was greater than the value determined in the present study. The result of this comparison

demonstrates the variation of reported values are expectedly due to differences in experimental conditions. However, differences are shown by a comparison of data from similar experimental conditions, which would not be expected.

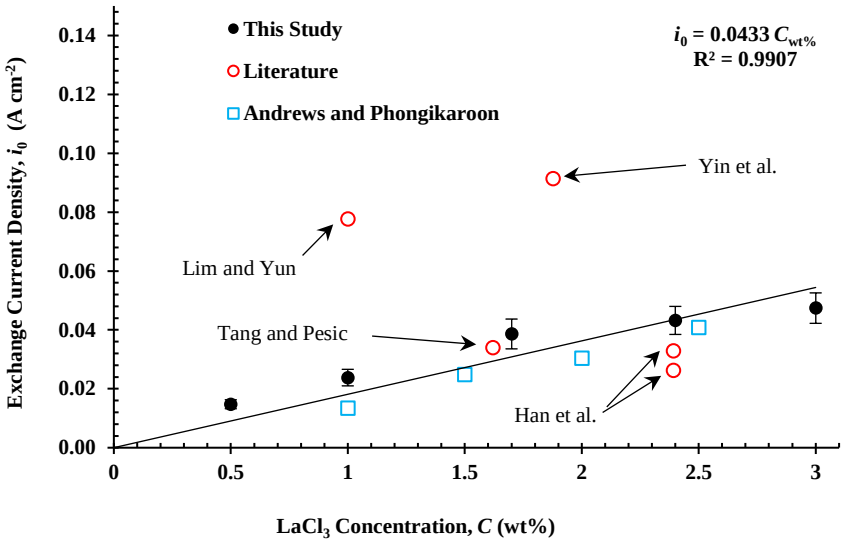

Figure 9. Exchange current density (i_0) as a function of the wt% concentration ($C_{wt\%}$) of $LaCl_3$ in ClLiK at 773 K. The error bars indicate standard deviations. Literature values are included for comparison.

Table 4. List of the range, average (μ), standard deviation (σ), coefficient of variation (c_v), and number of values (N) for $i_0 \times 10^2$ A cm^{-2} at the various concentrations of $LaCl_3$.

wt% $LaCl_3$	0.5	1.0	1.7	2.4	3.0
Range	1.15-1.71	1.66-2.80	2.51-4.66	3.09-6.37	3.63-5.44
μ	1.48	2.38	3.86	4.32	4.73
σ	0.153	0.281	0.507	0.476	0.516
c_v	0.103	0.118	0.131	0.110	0.109
N	42	39	33	42	45

Theoretically, R_{ct} is inversely proportional to i_0, and i_0 is directly proportional to $LaCl_3$ concentration ($C_{wt\%}$). While the observed relationships of i_0 vs. R_{ct}^{-1} and i_0 vs. $C_{wt\%}$ are not perfectly linear, they are monotonic when considering the average value, as shown in Figure 10 and Figure 11, respectively. Here again, the standard deviations are indicated by error bars, and in this case, averages of R_{ct} range from 0.404 to 1.99 Ω, and Table 5 lists the range, μ, σ, c_v and N. Values of R_{ct} seem to be less commonly found in the literature and vary based on the electrochemical system and technique applied (e.g., direct or alternating current) to perform experiments. Reports of values found of $LaCl_3$ were in the range from 0.059 to 0.8 Ω and in general are smaller than those obtained in the present study. Yang et al. [35] utilized aluminum and gallium liquid WE at 773 K, and for 1.9 wt% $LaCl_3$ the values of R_{ct} as determined by EIS modeling were 0.256 and 0.0753 Ω, respectively. Han et al. [6] calculated R_{ct} using the Tafel method at low overpotentials under the same conditions as those described for exchange current density estimations. By an extrapolation of the R_{ct} vs. T data, the value of R_{ct} at 773 K was 0.625 Ω, which is slightly higher than that of the present study at the same concentration. Vandarkuzhali et al. [15] calculated a value of 0.78 Ω for R_{ct} at 1.13 wt% $LaCl_3$ and 748 K. This value of R_{ct} is lower than that of the present study (1.0 wt% at 773 K), yet it seems reasonable when a slightly higher concentration and significantly larger difference in temperature is considered. Yin et al. [32] calculated R_{ct} to be 0.243 Ω via EIS modeling methods, which is significantly smaller than what would be estimated based on results of the present study.

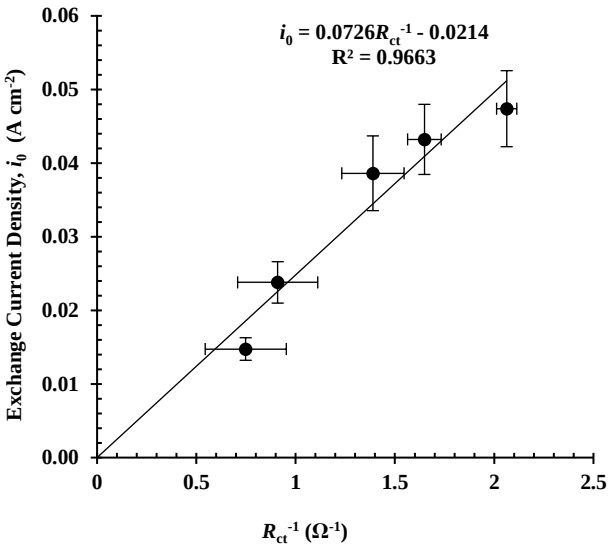

Figure 10. Exchange current density (i_0) vs. the inverse of charge transfer coefficient (R_{ct}). Error bars indicate standard deviations.

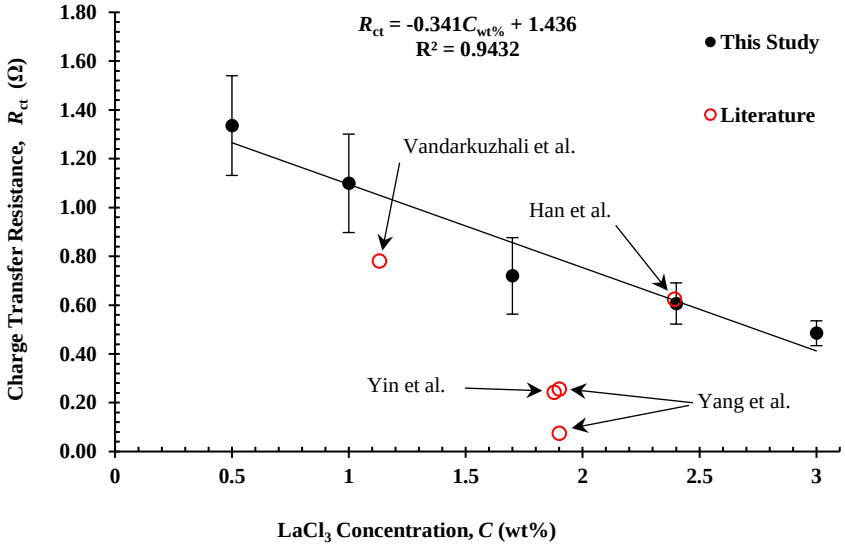

Figure 11. Charge transfer resistance (R_{ct}) vs. wt% concentration ($C_{wt\%}$) of $LaCl_3$ in ClLiK at 773 K. The error bars indicate standard deviations. Literature values are included for comparison. It is noted the value reported by Vandarkuzhali et al. [15] shown on the plot was estimated via data obtained at 748 K and that of Han et al. [6] was extrapolated to 773 K.

Table 5. List of the range, average (μ), standard deviation (σ), coefficient of variation (c_v), and number of values (N) for R_{ct} (Ω) at the various concentrations of $LaCl_3$.

wt% $LaCl_3$	0.5	1.0	1.7	2.4	3.0
Range	1.08-1.99	0.813-1.66	0.560-1.14	0.478-0.793	0.404-0.591
μ	1.34	1.10	0.719	0.607	0.484
σ	0.204	0.202	0.157	0.0844	0.0509
c_v	0.152	0.184	0.218	0.139	0.105
N	42	39	33	42	45

5. Conclusions

An analysis of CV data generated from testing of $LaCl_3$ in a range of concentrations in ClLiK was performed at 773 K. The reduction process of lanthanum ions in the molten salt was determined to be diffusion controlled, which agrees with reports published in the literature. The soluble-insoluble reaction was deemed to be irreversible in nature. Tafel analysis was applied to the charge transfer controlled region within the anodic sweep of the CV where the net current is zero, whereby the equilibrium potential (E_{eq}) was identified. Theoretical equations were applied to the CV data to estimate the values of α, D, i_0, and R_{ct}. Overall, the average value of α was 0.262. The overall average value of D was 1.67×10^{-5} cm^2 s^{-1} and values at each concentration of $LaCl_3$ in the electrolyte increased linearly. The magnitude of i_0 was observed to increase linearly with $LaCl_3$ concentration, with a calculated proportionality constant of 0.0435. The expected inverse proportionality between i_0 and R_{ct} was observed with R_{ct} decreasing linearly with $LaCl_3$ concentration. R_{ct} ranged from 0.404 to 1.99 Ω and i_0 ranged from 0.0148 to 0.0473 A cm^{-2}. In general, the values of D, i_0, and R_{ct} published in the literature were not only observed to be largely varied, but also dissimilar when compared to those of the present study. This was most likely due to differences in such experimental conditions as electrode materials and applied electrochemical technique. Overall, the impact of this research was to determination of parameters among a relatively large range of concentrations enabling comparison to those available in literature.

Acknowledgments

The authors gratefully acknowledge the operational support received from Kristi Moser-McIntire (Idaho State University), Joanna Taylor (University of Idaho), and Paul Smith (Idaho National Laboratory) at the Center of Advanced Energy Studies.

Conflict of interest

The authors declare that they have no known competing financial interests or personal relationships that could have appeared to influence the work reported in this paper. This manuscript was authored by Battelle Energy Alliance, LLC, under U.S. Department of Energy Contract No. DE–AC07–05ID14517. The U.S. Government retains and the publisher, by accepting the article for publication, acknowledges that the U.S. Government retains a nonexclusive, paid-up, irrevocable, worldwide license to publish or reproduce the published form of this manuscript, or allow others to do so, for U.S. Government purposes.

U.S. Department of Energy disclaimer

This information was prepared as an account of work sponsored by an agency of the U.S. Government. Neither the U.S. Government nor any agency thereof, nor any of their employees, makes any warranty, express or implied, or assumes any legal liability or responsibility for the accuracy, completeness, or usefulness of any information, apparatus, product, or process disclosed, or represents that its use would not infringe privately owned rights. References herein to any specific commercial product, process, or service by trade name, trademark, manufacturer, or otherwise, does not necessarily constitute or imply its endorsement, recommendation, or favoring by the U.S. Government or any agency thereof. The views and opinions of authors expressed herein do not necessarily state or reflect those of the U.S. Government or any agency thereof.

References

[1] Macdonald, D.D. Transient Techniques in Electrochemistry. **1977**, https://doi.org/10.1007/978-1-4613-4145-1.
[2] Choi, E.-Y.; Jeong, S.M. Electrochemical processing of spent nuclear fuels: An overview of oxide reduction in pyroprocessing technology. *Prog. Nat. Sci.* **2015**, *25*, 572–582, https://doi.org/10.1016/j.pnsc.2015.11.001.
[3] Simpson, M.F.; Law, J.D. Nuclear Fuel, Reprocessing of. **2012**, 153–173, https://doi.org/10.1007/978-1-4614-5716-9_5.
[4] Till, C.; Chang, Y.; Hannum, W. The intergral fast reactor-an overview. *Prog. Nucl. Energy* **1997**, *31*, 3–11, https://doi.org/10.1016/0149-1970(96)00001-7.

[5] Nichols, A.L.; Aldama, D.L.; Verpelli, M. Handbook of Nuclear Data for Safeguards. Vienna, Austria; 2007. Available online: http://www-nds.iaea.org/reports-new/indc-reports/indc-nds/indc-nds-0534.pdf (accessed on 17 December 2022)
[6] Han, W.; Wang, W.; Li, M.; Wang, D.; Li, H.; Chen, J., et al. Electrochemical separation of La from LiCl-KCl fused salt by forming La-Pb alloys. Sep Purif Technol. 2021 Nov;275:119188. Available online: https://linkinghub.elsevier.com/retrieve/pii/S1383586621008984 (accessed on 17 December 2022)
[7] Ackerman, J.P.; Settle, J.L. Partition of lanthanum and neodymium metals and chloride salts between molten cadmium and molten LiCl-KCl eutectic. *J Alloys Compd* **1991**, *177*, 129–141. Available online: https://linkinghub.elsevier.com/retrieve/pii/0925838891900632 (accessed on 17 December 2022)
[8] Castrillejo, Y.; Bermejo, M.R.; Martínez, A.M.; Díaz, A. Electrochemical behavior of lanthanum and yttrium ions in two molten chlorides with different oxoacidic properties: The eutectic LiCl-KCl and the equimolar mixture CaCl2-NaCl. *J Min Metall Sect B Metall* **2003**, *39*, 109–135. Available online: http://www.doiserbia.nb.rs/Article.aspx?ID=1450-53390302109C (accessed on 17 December 2022)
[9] Tang, H.; Pesic, B. Electrochemical behavior of LaCl3 and morphology of La deposit on molybdenum substrate in molten LiCl–KCl eutectic salt. *Electrochimica Acta* **2014**, *119*, 120–130, https://doi.org/10.1016/j.electacta.2013.11.148.
[10] Lantelme, F.; Berghoute, Y. Electrochemical Studies of LaCl3 and GdCl3 Dissolved in Fused LiCl-KCl. *J. Electrochem. Soc.* **1999**, *146*, 4137–4144, https://doi.org/10.1149/1.1392604.
[11] Rappleye, D.; Jeong, S.-M.; Simpson, M. Electroanalytical Measurements of Binary-Analyte Mixtures in Molten LiCl-KCl Eutectic: Gadolinium(III)- and Lanthanum(III)-Chloride. *J. Electrochem. Soc.* **2016**, *163*, B507–B516, https://doi.org/10.1149/2.1011609jes.
[12] Gao, F.; Wang, C.; Liu, L.; Guo, J.; Chang, S.; Chang, L., et al. Electrode process of La(III) in molten LiCl-KCl. *J Rare Earths* **2009**, *27*, 986–990. Available online: https://linkinghub.elsevier.com/retrieve/pii/S1002072108603750 (accessed on 17 December 2022)
[13] Picard, G.; Mottot, Y.; Trémillon, B. Acidic and Redox Properties of Some Lanthanide Ions in Molten LiCl-KCl Eutectic. *ECS Proc. Vol.* **1986**, *1986-1*, 189–204, https://doi.org/10.1149/198601.0189pv.
[14] Masset, P.; Konings, R.J.; Malmbeck, R.; Serp, J.; Glatz, J.-P. Thermochemical properties of lanthanides (Ln=La,Nd) and actinides (An=U,Np,Pu,Am) in the molten LiCl–KCl eutectic. *J. Nucl. Mater.* **2005**, *344*, 173–179, https://doi.org/10.1016/j.jnucmat.2005.04.038.
[15] Vandarkuzhali, S.; Gogoi, N.; Ghosh, S.; Reddy, B.P.; Nagarajan, K. Electrochemical behaviour of LaCl3 at tungsten and aluminium cathodes in LiCl–KCl eutectic melt. *Electrochimica Acta* **2012**, *59*, 245–255, https://doi.org/10.1016/j.electacta.2011.10.062.
[16] Matsumiya, M.; Matsumoto, S. Electrochemical Studies on Lanthanum Ions in Molten LiCl-KCl-eutectic Mixture. *Zeitschrift für Naturforsch A* **2004**, *59*, 711–714. Available online: https://www.degruyter.com/document/doi/10.1515/zna-2004-1015/html (accessed on 17 December 2022)
[17] Bagri, P.; Simpson, M.F. Determination of activity coefficient of lanthanum chloride in molten LiCl-KCl eutectic salt as a function of cesium chloride and lanthanum chloride concentrations using electromotive force measurements. *J Nucl Mater* **2016**, *482*, 248–256. Available online: https://linkinghub.elsevier.com/retrieve/pii/S0022311516303920 (accessed on 17 December 2022)
[18] Guo, S.; Wu, E.; Zhang, J. Investigation of electrochemical kinetics for La(III)/La reaction in molten LiCl KCl eutectic salt using potentiometric polarization. *J Nucl Mater* **2018**, 510, 414–420. Available online: https://linkinghub.elsevier.com/retrieve/pii/S0022311518307967 (accessed on 17 December 2022)
[19] Samin, A.; Wang, Z.; Lahti, E.; Simpson, M.; Zhang, J. Estimation of key physical properties for LaCl3 in molten eutectic LiCl–KCl by fitting cyclic voltammetry data to a BET-based electrode reaction kinetics model. *J. Nucl. Mater.* **2016**, *475*, 149–155, https://doi.org/10.1016/j.jnucmat.2016.04.002.
[20] Kato, T.; Inoue, T.; Iwai, T.; Arai, Y. Separation behaviors of actinides from rare-earths in molten salt electrorefining using saturated liquid cadmium cathode. *J. Nucl. Mater.* **2006**, *357*, 105–114, https://doi.org/10.1016/j.jnucmat.2006.06.003.
[21] Serp, J.; Lefebvre, P.; Malmbeck, R.; Rebizant, J.; Vallet, P.; Glatz, J.-P. Separation of plutonium from lanthanum by electrolysis in LiCl–KCl onto molten bismuth electrode. *J. Nucl. Mater.* **2005**, *340*, 266–270, https://doi.org/10.1016/j.jnucmat.2004.12.004.
[22] Pang, J.-W.; Liu, K.; Liu, Y.-L.; Nie, C.-M.; Luo, L.-X.; Yuan, L.-Y.; Chai, Z.-F.; Shi, W.-Q. Electrochemical Properties of Lanthanum on the Liquid Gallium Electrode in LiCl-KCl Eutectic. *J. Electrochem. Soc.* **2016**, *163*, D750–D756, https://doi.org/10.1149/2.0611614jes.
[23] Smolenski, V.; Novoselova, A.; Osipenko, A.; Maershin, A. Thermodynamics and separation factor of uranium from lanthanum in liquid eutectic gallium-indium alloy/molten salt system. *Electrochimica Acta* **2014**, *145*, 81–85, https://doi.org/10.1016/j.electacta.2014.08.081.

[24] Ji, D.-B.; Yan, Y.-D.; Zhang, M.-L.; Li, X.; Jing, X.-Y.; Han, W.; Xue, Y.; Zhang, Z.-J. Separation of lanthanum from samarium on solid aluminum electrode in LiCl–KCl eutectic melts. *J. Radioanal. Nucl. Chem.* **2015**, *304*, 1123–1132, https://doi.org/10.1007/s10967-015-3978-8.
[25] Serp, J.; Allibert, M.; Le Terrier, A.; Malmbeck, R.; Ougier, M.; Rebizant, J.; Glatz, J.-P. Electroseparation of Actinides from Lanthanides on Solid Aluminum Electrode in LiCl-KCl Eutectic Melts. *J. Electrochem. Soc.* **2005**, *152*, C167–C172, https://doi.org/10.1149/1.1859812.
[26] Shaltry, M.R.; Allahar, K.N.; Butt, D.P.; Simpson, M.F.; Phongikaroon, S. Electrochemical Impedance Spectroscopy and Cyclic Voltammetry Methods for Monitoring SmCl3 Concentration in Molten Eutectic LiCl-KCl. *J Nucl Fuel Cycle Waste Technol* **2020** ,18, 1–18. Available online: http://www.jnfcwt.or.kr/journal/article.php?code=70600 (accessed on 17 December 2022)
[27] Bard, A.J.; Faulkner, L.R. Electrochemical Methods: Fundamentals and Applications. 2nd Ed. New York: Wiley; 2001. p833.
[28] Yoon, D.; Phongikaroon, S. Measurement and Analysis of Exchange Current Density for U/U3+ Reaction in LiCl-KCl Eutectic Salt via Various Electrochemical Techniques. *Electrochim Acta* **2017**, *227*, 170–179. Available online: https://linkinghub.elsevier.com/retrieve/pii/S0013468617300117 (accessed on 17 December 2022)
[29] Shaltry, M.R.; Hoover, R.O.; Fredrickson, G.L. Kinetic Parameters and Diffusivity of Uranium in FLiNaK and ClLiK. *J. Electrochem. Soc.* **2020**, *167*, 116502, https://doi.org/10.1149/1945-7111/ab9ef0.
[30] Boyle, D.T.; Kong, X.; Pei, A.; Rudnicki, P.E.; Shi, F.; Huang, W.; Bao, Z.; Qin, J.; Cui, Y. Transient Voltammetry with Ultramicroelectrodes Reveals the Electron Transfer Kinetics of Lithium Metal Anodes. *ACS Energy Lett.* **2020**, *5*, 701–709, https://doi.org/10.1021/acsenergylett.0c00031.
[31] Gao, F.; Wang, C.; Liu, L.; Guo, J.; Chang, S.; Chang, L.; et al. Electrode process of La(III) in molten LiCl-KCl. *J Rare Earths* **2009**, *27*, 986–990. Available online: https://linkinghub.elsevier.com/retrieve/pii/S1002072108603750 (accessed on 17 December 2022)
[32] Yin, T.-Q.; Liu, Y.; Yang, D.; Yan, Y.; Wang, G.; Chai, Z.; Shi, W. Thermodynamics and Kinetics Properties of Lanthanides (La, Ce, Pr, Nd) on the Liquid Bismuth Electrode in LiCl-KCl Molten Salt. *J. Electrochem. Soc.* **2020**, *167*, https://doi.org/10.1149/1945-7111/abb0f4.
[33] Andrews, H.; Phongikaroon, S. Comparison of Exchange Current Density Acquisition Methods for $LaCl_3$in Molten LiCl-KCl Eutectic Salt. *J. Electrochem. Soc.* **2018**, *165*, E412–E419, https://doi.org/10.1149/2.0041810jes.
[34] Lim, K.H.; Yun, J.I. Study on the exchange current density of lanthanide chlorides in LiCl-KCl molten salt. *Electrochim Acta* **2019**, *295*, 577–583. Available online: https://linkinghub.elsevier.com/retrieve/pii/S0013468618323442 (accessed on 17 December 2022)
[35] Yang, D.-W.; Jiang, S.-L.; Liu, Y.-L.; Yin, T.-Q.; Li, M.; Wang, L.; Luo, W.; Chai, Z.-F.; Shi, W.-Q. Electrodeposition Mechanism of La^{3+} on Al, Ga and Al-Ga Alloy Cathodes in LiCl-KCl Eutectic Salt. *J. Electrochem. Soc.* **2021**, *168*, 062511, https://doi.org/10.1149/1945-7111/ac0aa9.